

# $^{19}\text{F}$ , $^{13}\text{C}$ Correlations in a Highly Fluorinated Alkyl Chain and Coupling Constant Signs at the Fluorocarbon/Hydrocarbon Interface

Anthony A. Ribeiro\*

Duke NMR Spectroscopy Center and Department of Radiology, B143 Levine Science Research Center, Box 3711, Duke University Medical Center, Durham, North Carolina 27710, USA

The first  $^{19}\text{F}$ ,  $^{13}\text{C}$  HMQC correlations with full carbon decoupling and the first HMBC correlations using fluorine detection methods are reported, and combined with  $^{19}\text{F}$ -decoupled  $^{13}\text{C}$  data and  $^{19}\text{F}$ ,  $^{19}\text{F}$  COSY and TOCSY to derive the  $^{19}\text{F}$  and  $^{13}\text{C}$  assignments for the highly fluorinated alkanol 8,8,8 7,7 6,6 5,5 4,4 3,3-tridecafluorooctan-1-ol. The analyses of unique sets of multiple  $^{19}\text{F}$ ,  $^{13}\text{C}$  and  $^1\text{H}$ ,  $^{13}\text{C}$  cross peaks provides information about the relative signs of the coupling constants at the fluorocarbon/hydrocarbon interface.

*Magn. Reson. Chem.* 35, 215–221 (1997) No. of Figures: 5 No. of Tables 2 No. of References: 34

**Keywords:** NMR;  $^{19}\text{F}$  NMR;  $^{13}\text{C}$  NMR;  $^{19}\text{F}$ ,  $^{13}\text{C}$  correlations;  $^{19}\text{F}$  decoupling;  $^{13}\text{C}$ ,  $^1\text{H}$  coupling constants;  $^{13}\text{C}$ ,  $^{19}\text{F}$  coupling constants; fluorinated octanol

Received 1 July 1996; accepted 6 September 1996

## INTRODUCTION

Fluorinated alkyl compounds have exceptional abilities to dissolve gases such as oxygen.<sup>1,2</sup> They find application as blood substitutes,<sup>3</sup> breathing media in lungs and monitors of oxygen tension in tissues<sup>4,5</sup> and tumors.<sup>6</sup>

In the absence of fluorine decoupling, the  $^{13}\text{C}$  NMR spectra of perfluorinated or highly fluorinated alkyl chains are very complex. The chemical shifts of the fluorinated carbon nuclei are very near to one another, and the  $^{13}\text{C}$  resonances are split by multi-bond  $^{19}\text{F}$ – $^{13}\text{C}$  couplings. There are further splittings from  $^1\text{H}$ – $^{13}\text{C}$  couplings in the case of highly fluorinated compounds. This is shown in the fully coupled  $^{13}\text{C}$  NMR spectrum [Fig. 1(A)] of the highly fluorinated alkanol 8,8,8 7,7 6,6 5,5 4,4 3,3 tridecafluorooctan-1-ol (1).



1

At 125 MHz, the six fluorinated carbons (C-3–C-8) give rise to >57 resolved lines in a 16 ppm region between 106 and 122 ppm due to one-, two- and possibly three-bond fluorine–carbon couplings as well as multi-bond proton–carbon couplings from the protonated methylene groups. The C-2 methylene appears at 34.3 ppm as a nine-line triplet of triplets with a one-bond proton–carbon coupling of *ca.* 130 Hz and a two-bond fluorine–carbon coupling of *ca.* 21 Hz. The C-1 methylene resonates at 55.0 ppm as a second triplet of triplets with a one-bond proton–carbon coupling of *ca.*

145 Hz and an additional small coupling of *ca.* 5 Hz, which is taken as a two-bond proton–carbon coupling. In a previous study,<sup>7</sup> we devised two strategies based on  $^1\text{H}$ ,  $^{13}\text{C}$  correlations to obtain a spectral simplification of the fluorinated chain of 1. Using one-dimensional (1D) selective INEPT and two-dimensional (2D) NMR, we spectrally selected nine out of the >57 resolved lines between 106 and 122 ppm and identified these lines as arising from the C-3  $\text{CF}_2$  moiety.

The NMR analysis of 1 is completed here using homonuclear  $^{19}\text{F}$ ,  $^{19}\text{F}$  2D NMR,  $^{19}\text{F}$ -decoupled  $^{13}\text{C}$  1D NMR and heteronuclear  $^{19}\text{F}$ ,  $^{13}\text{C}$  2D NMR correlation methods. We are aware of only three papers<sup>8–10</sup> that have explored  $^{19}\text{F}$ ,  $^{13}\text{C}$  2D correlations. We previously reported the first single- and multi-bond  $^{19}\text{F}$ ,  $^{13}\text{C}$  correlations using  $^{13}\text{C}$  detection methods.<sup>8</sup> Bourdonneau and Brevard<sup>9</sup> and Berger<sup>10</sup> have used  $^{19}\text{F}$  detection to record single-bond  $^{19}\text{F}$ ,  $^{13}\text{C}$  correlations based on the HMQC method<sup>11</sup> without  $^{13}\text{C}$  decoupling. Here we report the first fluorine-detected single- and multi-bond correlations based on the HMQC method with full  $^{13}\text{C}$  decoupling<sup>11,12</sup> and on the HMBC technique<sup>12,13</sup> to complete the  $^{13}\text{C}$  and  $^{19}\text{F}$  NMR assignments in 1. In addition, we have determined the relative signs of the coupling constants at the interface of the fluorinated and protonated portions of 1 by analyses of unique sets of multiple 2D cross peaks.

## EXPERIMENTAL

The perfluoroalkanol 1 was purchased from Aldrich Chemical (St Louis, MO, USA) and was used without further purification. NMR data were recorded on a sealed sample of 80% (v/v) of 1 in  $\text{C}_6\text{D}_6$  in a 5 mm

\* Correspondence to: A. A. Ribeiro.

Contract grant sponsor: NIH; Contract grant numbers: NCI P30-CA-14326.

NMR tube at 28 °C using a Varian Unity 500 spectrometer. NMR spectra were recorded using a 5 mm Varian inverse probe with the high-band coil tuned for  $^{19}\text{F}$  resonance at 470.38 MHz and the low-band coil tuned for  $^{13}\text{C}$  resonance at 125.72 MHz. The  $^{19}\text{F}$  90° pulse was 8  $\mu\text{s}$ . The  $^{19}\text{F}$  1D NMR spectra were recorded between -84 and -135 ppm using a 25 873 Hz spectral window digitized into 100 032 points. We used this same spectral window with 4K points for 2D COSY<sup>14,15</sup> and TOCSY<sup>16</sup> and with 2K points for the 2D HMQC and HMBC experiments.

COSY spectra were recorded in the absolute value mode; 600 time increments were collected and zero-filled to 4096 points with sine-bell weighting along both dimensions. Sixteen scans were collected per increment and the relaxation delay was 1 s. TOCSY spectra were collected in the phase-sensitive mode using two sets of 256 time increment spectra with Gaussian weighting in both dimensions, 16 scans per time increment, 1 s delay and 70 ms mixing time.

The  $^{13}\text{C}$  90° pulse was 10  $\mu\text{s}$ . 1D  $^{13}\text{C}$  NMR spectra were recorded between 20 and 140 ppm using a 15 089 Hz spectral window digitized into 128 000 points. The  $^{19}\text{F}$  decoupler was calibrated directly on the  $^{19}\text{F}$ -coupled  $\text{CF}_3$  resonance (C-8) of **1**, which is a clear quadruplet of triplets with  $^1J_{\text{CF}} \approx 287$  Hz centered at about 118.1 ppm [Fig. 1(A)]. Off-resonance decoupling gave reduced values of  $^1J_{\text{CF}}$  which were used to obtain  $\gamma_{\text{H}_2}/2\pi$  at various decoupler power values. GARP1<sup>17</sup> and WALTZ<sup>18,19</sup> decoupling gave  $\gamma_{\text{H}_2}/2\pi$  fields of >32 kHz which were adequate to decouple the  $\text{CF}_3$  and  $\text{CF}_2$   $^{19}\text{F}$  regions simultaneously.

Single-bond  $^{19}\text{F}$ ,  $^{13}\text{C}$  heteronuclear chemical shift correlation spectra were recorded in the inverse mode using  $^{19}\text{F}$  detection based on the HMQC<sup>11,12</sup> method with  $^{13}\text{C}$  decoupling using GARP1.<sup>17</sup> A BIRD filter was used to obtain better suppression of unwanted signals. Two sets of 300 time increments were obtained in the phase-sensitive mode, processed using Gaussian functions, and zero-filled to a final size of 2K  $\times$  2K. The relaxation delay was 1.2 s with 32 transients per increment.

Fluorine-detected multiple bond correlation spectra (HMBC) were recorded in the phase-sensitive mode without  $^{13}\text{C}$  decoupling during acquisition.<sup>12,13</sup> The HMBC spectra were plotted in mixed mode [absolute value in  $f_2$  ( $^{19}\text{F}$ ) and phase sensitive in  $f_1$  ( $^{13}\text{C}$ )]. A shifted Gaussian weighting function was used along  $f_2$  and a cosine weighting function was used along  $f_1$ . Two sets of 274 time increments were zero-filled to a final size of 2K  $\times$  2K. The relaxation delay was 1.2 s, the filter delay corresponded to an average  $^1J_{\text{CF}}$  of 275 Hz and 64 transients were obtained per increment. The long range  $^{19}\text{F}$ - $^{13}\text{C}$  couplings were allowed to evolve for a delay of 15 ms.

## RESULTS AND DISCUSSION

The 470 MHz  $^{19}\text{F}$  NMR spectrum of **1** reveals the single perfluoromethyl ( $\text{CF}_3$ ) and five perfluoromethylene ( $\text{CF}_2$ ) groups to resonate as six distinct  $^{19}\text{F}$  signals between -85 and -130 ppm (Fig. 2). The -85.6 ppm

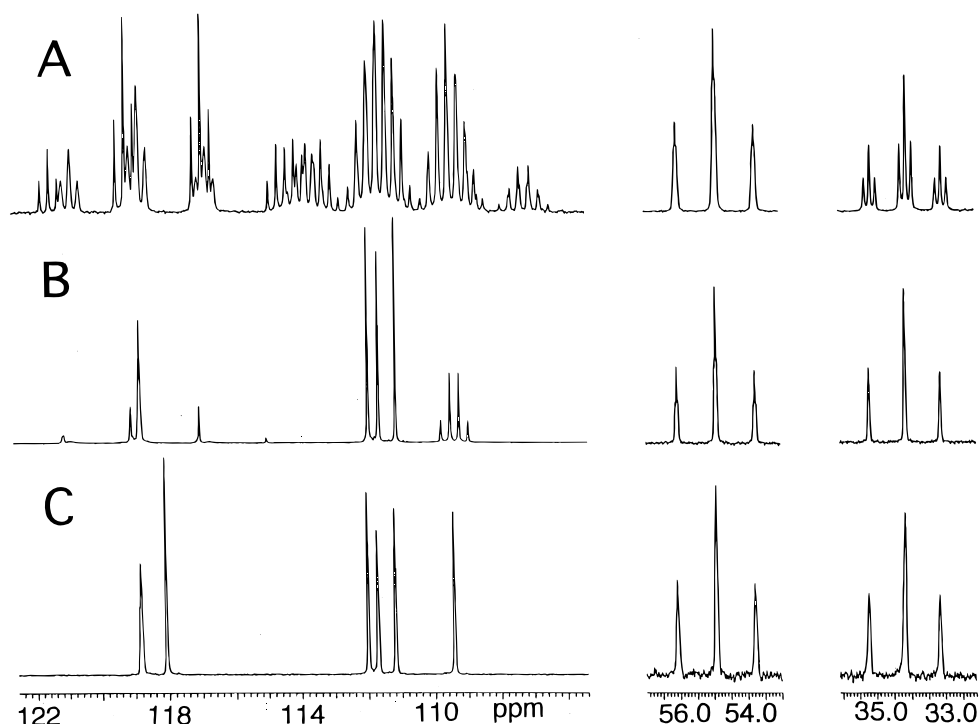


**Figure 1.** Expansions of 125 MHz  $^{13}\text{C}$  NMR spectra of the highly fluorinated octanol **1** in  $\text{C}_6\text{D}_6$ . (A)  $^{13}\text{C}$  NMR multiplets in the presence of  $^{19}\text{F}$ - $^{13}\text{C}$  and  $^1\text{H}$ - $^{13}\text{C}$  coupling, 2048 scans. C-3–C-8 give rise to >57 lines between 122 and 106 ppm. C-1 is the 'triplet of triplets' near 55.0 ppm and C-2 is the 'triplet of triplets' near 34.3 ppm. (B)  $^{13}\text{C}$  NMR spectrum with  $^{19}\text{F}$  decoupling of the  $\text{CF}_2$  signals, 400 scans. The singlets arise from C-4–C-6. The 118.1 ppm quartet with  $^1J_{\text{FC}}$  arises from C-8. The 109.4 ppm quartet with  $^2J_{\text{FC}}$  arises from C-7. The triplet at 118.8 ppm with  $^2J_{\text{HC}}$  arises from C-3. C-2 now appears similar to C-1. (C) With simultaneous  $^{19}\text{F}$  decoupling of the  $\text{CF}_2$  and  $\text{CF}_3$  groups, the  $^{13}\text{C}$  resonances simplify to singlets, except for C-3, which retains triplet character from  $^2J_{\text{HC}}$  coupling.

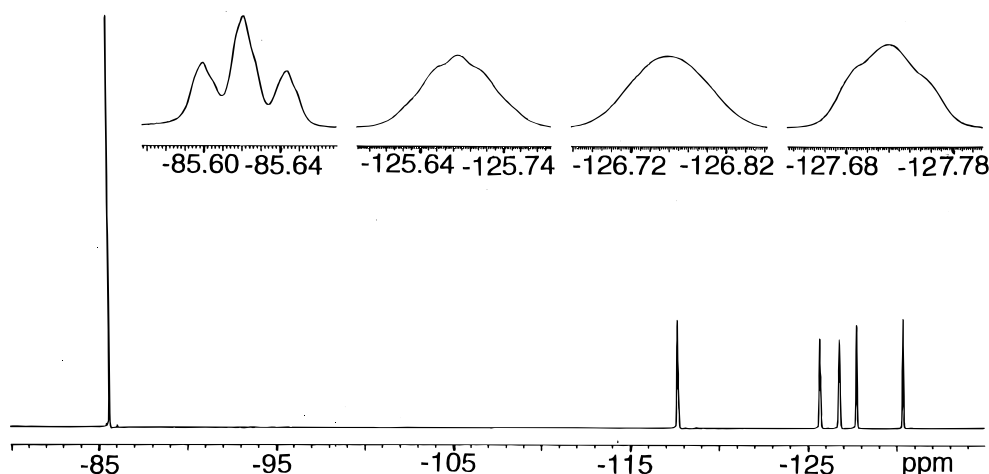


**Figure 2.** 470 MHz  $^{19}\text{F}$  NMR spectrum of the highly fluorinated octanol **1** in  $\text{C}_6\text{D}_6$  showing the  $\text{CF}_3$  signal at  $-85.6$  ppm and the  $\text{CF}_2$  resonances at  $-117$  to  $-131$  ppm with expansions of selected resonances (see text for details).

signal is assigned to C-8 ( $\text{CF}_3$ ) based on intensity and chemical shift/structural considerations. The  $\text{CF}_3$  signal is a triplet with unresolved couplings. The linewidth of the center line is *ca.* 6 Hz. The assignment of the  $\text{CF}_2$  signals is not obvious. The expansions reveal complex resonances with linewidths near 50 Hz and poorly resolved couplings. The  $-125.7$  and  $-127.7$  ppm  $\text{CF}_2$  multiplets (C-5 and C-4) show fine structure but the  $-126.8$  ppm multiplet (C-6) is a broad, featureless resonance with unresolvable couplings. This  $^{19}\text{F}$  spectrum of **1** is observed when the sample is well shimmed and the  $^1\text{H}$  resonances from the C-1 and C-2  $\text{CH}_2$  groups (Fig. 1 in Ref. 7) and the  $^{13}\text{C}$  signals (Fig. 1) are sharp with well resolved couplings and linewidths of 2–4 Hz.

The amplitude of cross peaks in COSY is known to depend on the  $T_2$  relaxation of the coupled nuclei, and not on  $T_2^*$ , which governs the effective linewidth of a resonance.<sup>15</sup> COSY thus has a very useful feature with an ability to detect spin–spin couplings between nuclei even when the coupling is not resolved.  $^{19}\text{F}$ ,  $^{19}\text{F}$  2D COSY has been used previously to explore couplings in

fluorinated alkyl chains.<sup>10,20</sup> The full and expanded  $^{19}\text{F}$ ,  $^{19}\text{F}$  2D COSY maps obtained experimentally for **1** are shown in Fig. 3(A) and (B). The  $\text{CF}_3$  resonance at  $-85.6$  ppm shows a strong cross peak to the  $-126.8$  ppm  $\text{CF}_2$  and a weak cross peak to the  $-125.7$  ppm  $\text{CF}_2$  line, while each  $\text{CF}_2$  resonance shows multiple off-diagonal connectivities. For example, the  $-125.7$  ppm  $\text{CF}_2$  resonance (arising from C-5) couples to all the other fluorinated moieties. The multiple cross peaks in the  $^{19}\text{F}$ ,  $^{19}\text{F}$  COSY of this linear fluoroalkyl chain are unusual compared with the results for the  $^1\text{H}$ ,  $^1\text{H}$  COSY of linear alkyl chains, e.g. the butyl group in amiodarone,<sup>21</sup> which only evidence the three-bond coupling between adjacent  $\text{CH}_2$  groups. The  $^{19}\text{F}$ ,  $^{19}\text{F}$  COSY result showing a complete network of spins for a linear chain is more similar to that expected from a TOCSY experiment. In fact, a phase-sensitive  $^{19}\text{F}$ ,  $^{19}\text{F}$  TOCSY experiment carried out with 70 ms mix time (not shown) resulted in a virtually identical 2D map as the COSY method. The results provide evidence that the  $^{19}\text{F}$ – $^{19}\text{F}$  couplings in **1** persist across three, four or five bonds.<sup>20</sup> The  $^3J_{\text{FF}}$ ,  $^4J_{\text{FF}}$  and  $^5J_{\text{FF}}$  couplings are

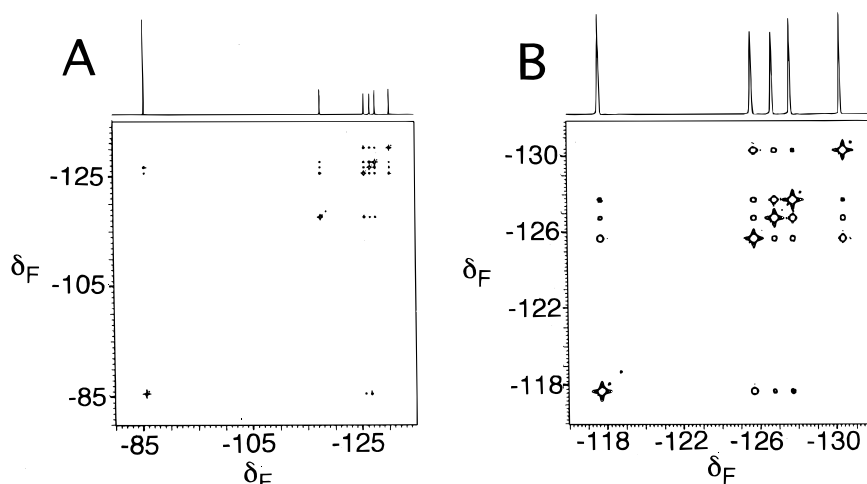


**Figure 3.** (A) 470 MHz 2D COSY map showing  $^{19}\text{F}$ – $^{19}\text{F}$  spin connectivities between  $\text{CF}_3$  and  $\text{CF}_2$  regions of the highly fluorinated alcohol **1** in  $\text{C}_6\text{D}_6$ . (B) Expanded 2D map showing connectivities within the  $\text{CF}_2$  region. Note the presence of dominant and weaker cross peaks arising from four- and three- or five-bond  $^{19}\text{F}$ – $^{19}\text{F}$  couplings.

detected by COSY despite being small relative to the linewidths of the  $^{19}\text{F}$  resonances.

The COSY expansion [Fig. 3(B)] reveals distinct dominant and weaker COSY cross peaks. For example, the connectivities from the  $-125.7$  ppm  $^{19}\text{F}$  signal (C-5) to the  $^{19}\text{F}$  resonances at  $-117.7$  and  $-130.35$  ppm are clearly stronger than the cross peaks to the  $^{19}\text{F}$  signals at  $-126.8$  and  $-127.7$  ppm. Since work on fluoropolymers<sup>20</sup> has shown  $^4J_{\text{FF}}$  usually to be larger than  $^3J_{\text{FF}}$  and  $^5J_{\text{FF}}$ , the dominant COSY connectivities are appropriately interpreted as arising from  $n, n+2$  couplings, i.e. between next-nearest neighbor groups. Using this view, the  $-85.6$  ppm ( $\text{CF}_3$ ),  $-126.8$  ppm ( $\text{CF}_2$ ) and  $-127.7$  ppm ( $\text{CF}_2$ ) signals can be assigned to C-8, C-6 and C-4, respectively. Also, the  $-125.7$  ppm signal is identified as C-5, and the  $-117.7$  and  $-130.35$  ppm  $\text{CF}_2$  signals are identified as the C-3–C-7 pair.

To put these tentative assignments on firmer ground, we explored the use of heteronuclear strategies.  $^{19}\text{F}$ ,  $^{13}\text{C}$  couplings are about double  $^1\text{H}$ ,  $^{13}\text{C}$  couplings, and  $^{19}\text{F}$  shifts occur over a wider spectral range than  $^1\text{H}$  shifts. On a 500 MHz NMR spectrometer, the separation between the  $\text{CF}_3$  and  $\text{CF}_2$  resonances is *ca.* 30 kHz. This is a factor of about six larger than the 5 kHz needed to span a 10 ppm  $^1\text{H}$  window. Thus, complete  $^{19}\text{F}$  decoupling is more difficult to achieve than complete  $^1\text{H}$  decoupling. Indeed, in early work with fluoroalkanes<sup>2,22,23</sup> using traditional noise decoupling methods, two separate  $^{13}\text{C}$  spectra needed to be recorded, first with the  $^{19}\text{F}$  decoupler set on the trifluoromethyl resonance (*ca.*  $-85$  ppm) and then at the mid-point of the perfluoromethylene resonances (*ca.*  $-120$  ppm). The successful recording of a single  $^{13}\text{C}$  spectrum for a fluoroalkane with complete  $^{19}\text{F}$  decoupling was achieved only with the use of very high power (50 W) decoupler units.<sup>2,23</sup> In the present study, we implement newer and more efficient broadband decoupling schemes such as GARP<sup>17</sup> or WALTZ<sup>18,19</sup> that use  $<2$  W of power to achieve complete  $^{19}\text{F}$  decoupling of  $\text{CF}_3$  and  $\text{CF}_2$  resonances.

When fluorine decoupling is applied simultaneously to the  $\text{CF}_3$  and  $\text{CF}_2$  regions, all the fluorinated carbon signals collapse to singlets [Fig. 1(C)], except for the perfluoromethylene resonance at 118.8 ppm, which is a triplet with a small two-bond  $^1\text{H}$ – $^{13}\text{C}$  coupling. This triplet is clearly the  $\text{CF}_2$  group from C-3 adjacent to the C-2  $\text{CH}_2$  in the hydrocarbon portion of **1**. This C-3 assignment agrees with the previous  $^1\text{H}$ ,  $^{13}\text{C}$  2D and selective INEPT results.<sup>7</sup> The two-bond  $^{19}\text{F}$  coupling to the C-2  $\text{CH}_2$  at 34.3 ppm is also removed, and this resonance collapses to a multiplet with mainly triplet character from a large one-bond  $^1\text{H}$ – $^{13}\text{C}$  coupling and a small two-bond  $^1\text{H}$ – $^{13}\text{C}$  coupling.

When the decoupler is set to decouple only the  $\text{CF}_2$  resonances, the  $^{13}\text{C}$  quadruplet of triplets centered at *ca.* 118.1 ppm in the fully coupled spectrum [Fig. 1(A)] collapses to a simple quartet with a one-bond  $^{19}\text{F}$ – $^{13}\text{C}$  coupling of 287 Hz [Fig. 1(B)] and is unequivocally identified as the C-8  $\text{CF}_3$  resonance. A second  $^{13}\text{C}$  quartet appears at 109.4 ppm with a two-bond  $^{19}\text{F}$ – $^{13}\text{C}$  coupling of *ca.* 34 Hz. This quartet clearly arises from the perfluoromethylene next to the  $\text{CF}_3$  group, i.e. the C-7  $\text{CF}_2$ . The C-3  $\text{CF}_2$  at 118.8 ppm is again a  $^{13}\text{C}$  triplet with a two-bond  $^1\text{H}$ – $^{13}\text{C}$  coupling.

$^{19}\text{F}$ ,  $^{13}\text{C}$  heteronuclear 2D NMR spectroscopy on fluoroalkanes is at present essentially unexplored. Figure 4(A) shows the expanded  $^{19}\text{F}$ ,  $^{13}\text{C}$  single bond (HMQC) shift correlation map for the five  $\text{CF}_2$  groups of **1** with corresponding 1D  $^{19}\text{F}$  and  $^{19}\text{F}$ -decoupled  $^{13}\text{C}$  spectra plotted on the top and side of the 2D map. Five single AX-type cross peaks are seen connecting the directly bonded perfluoromethylenes to their respective carbons. The 118.8 and 109.4 ppm  $^{13}\text{C}$  resonances were unequivocally identified as C-3 and C-7 by fluorine decoupling (above). The  $-117.7$  and  $-130.35$  ppm  $^{19}\text{F}$  resonances are therefore assigned to the C-3 and C-7  $\text{CF}_2$  groups from their respective direct correlations to those  $^{13}\text{C}$  signals. A similar direct correlation of the  $-85.6$  ppm  $^{19}\text{F}$  signal to the 118.1 ppm  $^{13}\text{C}$  signal (not shown) verifies its assignment to the C-8  $\text{CF}_3$  group.

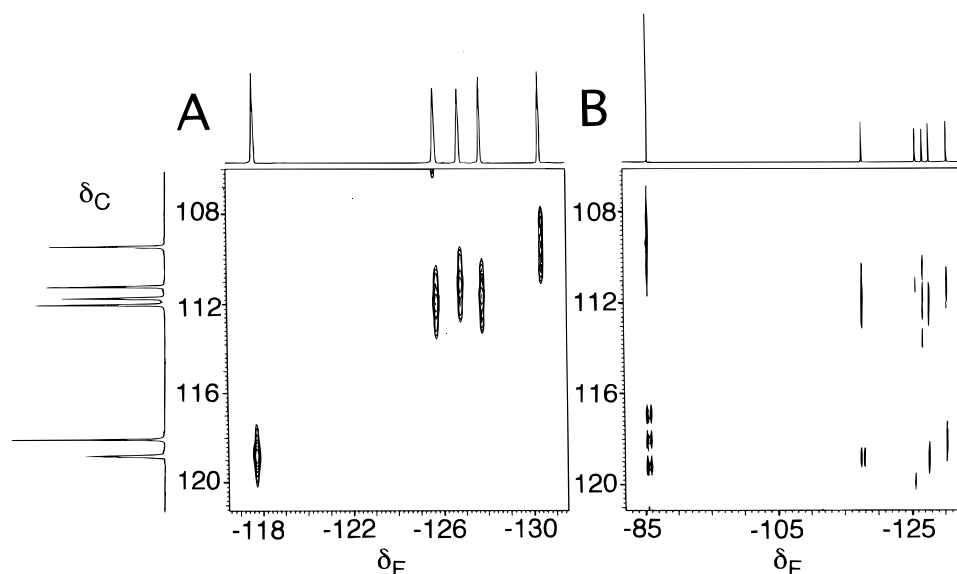


**Figure 4.** (A)  $^{19}\text{F}$ -detected 2D  $^{19}\text{F}$ – $^{13}\text{C}$  single-bond correlation (HMQC) of directly fluorinated carbons of the highly fluorinated alcohol **1** in  $\text{C}_6\text{D}_6$ . (B)  $^{19}\text{F}$ -detected 2D  $^{19}\text{F}$ – $^{13}\text{C}$  multi-bond correlation (HMBC) of **1** optimized for  $^2J_{\text{FC}}$  couplings of *ca.* 33 Hz. The responses from the  $\text{CF}_3$  at  $-85.6$  ppm show 'sinc wiggles' due to the weighting function in the data processing.

This leaves the three central perfluoromethylene groups (C-4–C-6) to be identified.

Figure 4(B) shows the corresponding multi-bond (HMBC)  $^{19}\text{F}$ ,  $^{13}\text{C}$  shift correlation map for the  $\text{CF}_3$  and  $\text{CF}_2$  regions with the 1D  $^{19}\text{F}$  NMR spectrum plotted on top of the 2D map. Using a 15 ms evolution time, direct and multi-bond responses are successfully elicited at four of the six  $^{19}\text{F}$  positions. For example, the C-3  $\text{CF}_2$  gives the  $^{19}\text{F}$ -coupled direct response at 118.8 ppm and a strong multi-bond cross peak to the 111.7 ppm  $^{13}\text{C}$  position which is recognized as the  $^2J_{\text{FC}}$  correlation to the C-4 carbon. The C-3  $\text{CF}_2$  also yields a strong  $^2J_{\text{FC}}$  response at the C-2 methylene (34.3 ppm) (see below). The C-7  $\text{CF}_2$  resonance at  $-130.35$  ppm elicits two strong connectivities at 111.2 and 118.1 ppm which are recognized as the  $^2J_{\text{FC}}$  responses to C-6 ( $\text{CF}_2$ ) and C-8 ( $\text{CF}_3$ ). The four multi-bond responses suffice for a full assignment. Only the  $^{13}\text{C}$  signal at 112.0 ppm remains to be assigned to C-5. Consistency of assignments is checked by using the direct correlation in HMQC from C-4 (111.7 ppm) to assign the  $-127.7$  ppm  $^{19}\text{F}$  signal to the C-4  $\text{CF}_2$ , and then going back in the HMBC results to locate the multi-bond responses at 118.8 ppm (C-3) and 112.0 ppm (C-5). The C-8  $\text{CF}_3$  resonance at  $-85.6$  ppm elicits a strong  $^2J_{\text{FC}}$  response at 109.4 ppm (C-7) and a  $^{19}\text{F}$ -coupled direct response at 118.1 ppm (C-8). At the conditions of the HMBC experiment, the  $-125.7$  and  $-126.8$  ppm  $^{19}\text{F}$  signals (from C-5 and C-6) showed streaking from noise and no successful multi-bond responses were observed at these  $^{19}\text{F}$  positions. However, a sufficient number of responses were obtained at the other  $^{19}\text{F}$  positions to derive the complete  $^{19}\text{F}$  and  $^{13}\text{C}$  assignments for **1** summarized in Table 1.

It has been known for some time that the relative signs of the NMR spin coupling constants for an AMX system of three coupled spins can be determined by 2D NMR spectroscopy.<sup>15,24</sup> The presence of a passive M spin creates two AX subspectra, each corresponding to the M spin in the  $\alpha$  or  $\beta$  state. The single AX cross peak normally observed in 2D experiments (e.g. Fig. 4) changes to a set of multiple cross peaks split by  $J_{\text{AM}}$  along one axis and by  $J_{\text{AX}}$  along the other axis. This

modulation of AX cross peaks by a passive M spin offers the opportunity to obtain the relative signs and magnitudes of the coupling constants in a simple manner. We and several others have exploited this phenomenon<sup>7,8,25–29</sup> to explore mutually coupled  $^{19}\text{F}$ ,  $^1\text{H}$  and  $^{13}\text{C}$  spins using single-bond heteronuclear correlation experiments with  $^1\text{H}$  and  $^{13}\text{C}$  as the active spins and  $^{19}\text{F}$  as the passive spin. More recently, we found that the multi-bond 2D correlation experiment allows the recording of multiple cross peak patterns that are not accessible by the single-bond experiments.<sup>8</sup> We also found that correlation experiments with  $^{19}\text{F}$  and  $^{13}\text{C}$  spins as the active spins and  $^1\text{H}$  as the passive spin gave access to other couplings relevant to the three-nucleus system. This combination of the single- and multi-bond experiments with either  $^{19}\text{F}$  or  $^1\text{H}$  as the passive M spin offers a novel, straightforward, yet powerful way to obtain complete coupling constant and spin information about the relevant three-spin system.

The detection of multiple cross peaks at the C-3  $\text{CF}_2$  or C-2  $\text{CH}_2$  of **1** serves as an example of these strategies as it offers the opportunity to gain information on the signs and magnitudes of the heteronuclear coupling constants at the interface of the fluorinated and protonated portions of **1**.<sup>7,8</sup> The strategies are illustrated by first examining the strong multi-bond cross peak obtained by  $^{19}\text{F}$ ,  $^{13}\text{C}$  correlation from the C-3  $\text{CF}_2$  to the C-2  $\text{CH}_2$ . Here  $^{19}\text{F}$  and  $^{13}\text{C}$  are the active AX spin pair while  $^1\text{H}$  is the passive M spin. This correlation appears at  $^{19}\text{F}$ ,  $^{13}\text{C} = -117.7, 34.3$  ppm on the 2D map [Fig. 5(A)], and is seen as a unique set of three cross peaks appearing between 33.0 and 35.4 ppm ( $^{13}\text{C}$ ) and  $-117.5$  and  $-117.8$  ppm ( $^{19}\text{F}$ ). The magnitudes and relative signs<sup>7,8</sup> of the heteronuclear splittings,  $^3J_{\text{HF}}$  and  $^1J_{\text{HC}}$ , can be measured directly from Fig. 5(A). A  $^3J_{\text{HF}}$  coupling of 18.7 Hz is obtained from the cross-peak spacing along the  $^{19}\text{F}$  axis and a  $^1J_{\text{HC}}$  coupling of 130 Hz is obtained from the spacing along the  $^{13}\text{C}$  axis. The highest frequency  $^{19}\text{F}$  cross peak near  $-117.6$  ppm (along  $f_2$ ) has the highest  $^{13}\text{C}$  frequency near 35.0 ppm (along  $f_1$ ), and the lowest frequency  $^{19}\text{F}$  cross peak near  $-117.1$  ppm has the lowest  $^{13}\text{C}$  frequency near 33.1 ppm. When processed with Varian software, the result appears as three cross peaks skewed with a positive slope. Because the cross peaks are shifted in the same direction along both the  $f_1$  and  $f_2$  axes, the signs of  $^3J_{\text{HF}}$  and  $^1J_{\text{HC}}$  can be taken to be the same.

Figure 5(B) shows the single-bond  $^1\text{H}$ ,  $^{13}\text{C}$  correlation at the C-2 methylene obtained in a  $^1\text{H}$ -detected HMQC experiment, i.e. at  $^1\text{H}$ ,  $^{13}\text{C} = 2.46, 34.3$  ppm. The  $^1\text{H}$  and  $^{19}\text{F}$  nuclei have reversed roles here.  $^1\text{H}$  and  $^{13}\text{C}$  are now the active AX spins and  $^{19}\text{F}$  serves as the passive M spin. The single-bond  $^1\text{H}$ ,  $^{13}\text{C}$  correlation is a set of three cross peaks appearing between 34.1 and 34.5 ppm ( $^{13}\text{C}$ ) and between 2.41 and 2.48 ppm ( $^1\text{H}$ ). A value of 18.7 Hz is obtained for  $^3J_{\text{HF}}$  from the spacing along the  $^1\text{H}$  axis and a value of 21 Hz is obtained for  $^2J_{\text{FC}}$  from the spacing along the  $^{13}\text{C}$  axis. The highest frequency  $^1\text{H}$  cross peak near 2.48 ppm has the highest  $^{13}\text{C}$  frequency near 34.5 ppm, and the lowest frequency  $^1\text{H}$  cross peak near 2.41 ppm has the lowest  $^{13}\text{C}$  frequency near 34.1 ppm. The result appears as three cross peaks tilted with a positive slope, indicating that the signs of  $^3J_{\text{HF}}$  and  $^2J_{\text{FC}}$  are the same.

**Table 1.**  $^{19}\text{F}$ ,  $^1\text{H}$  and  $^{13}\text{C}$  NMR assignments of  $\text{CF}_3(\text{CF}_2)_5\text{CH}_2\text{CH}_2\text{OH}^a$

Carbon	$^1\text{H}$ (ppm) <sup>b</sup>	$^{19}\text{F}$ (ppm) <sup>c</sup>	$^{13}\text{C}$ (ppm) <sup>d</sup>
C-1	3.94		54.994
C-2	2.46		34.345
C-3		$-117.700$	118.820
C-4		$-127.732$	111.725
C-5		$-125.699$	112.020
C-6		$-126.777$	111.199
C-7		$-130.350$	109.423
C-8		$-85.622$	118.074

<sup>a</sup> Data at 28 °C.

<sup>b</sup>  $^1\text{H}$  chemical shifts relative to internal TMS.

<sup>c</sup>  $^{13}\text{C}$  chemical shifts expressed on TMS scale by setting  $\text{C}_6\text{D}_6$  to 128 ppm.

<sup>d</sup>  $^{19}\text{F}$  chemical shifts expressed relative to  $\text{CFCl}_3$  scale by setting a 3% trifluoroacetic acid in  $\text{D}_2\text{O}$  solution to  $-76.0$  ppm.

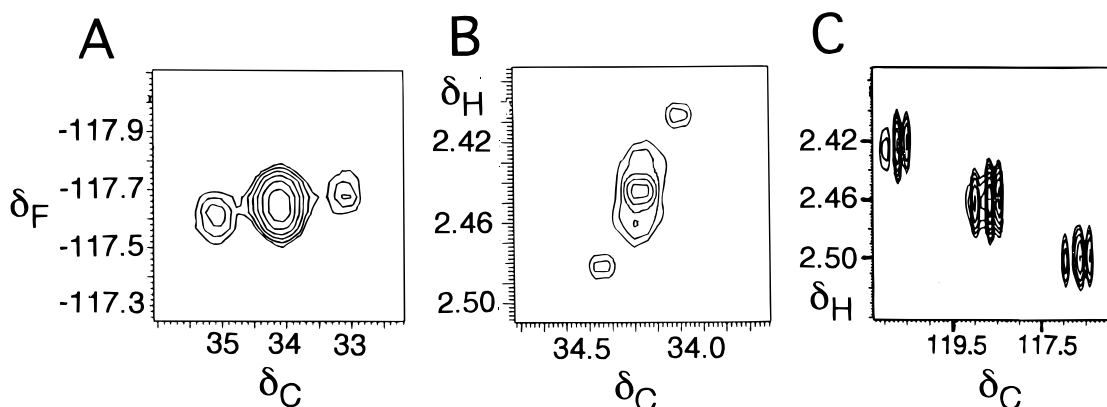


**Figure 5.** Sets of multiple cross peaks at the fluorocarbon/hydrocarbon interface of **1**. (A)  $^{19}\text{F}$ - $^{13}\text{C}$  multi-bond correlation at  $-117.7$ ,  $34.3$  ppm. (B)  $^1\text{H}$ - $^{13}\text{C}$  single-bond correlation at  $2.46$ ,  $34.3$  ppm. (C)  $^1\text{H}$ - $^{13}\text{C}$  multi-bond correlation at  $2.46$ ,  $118.8$  ppm.

Figure 5(C) shows the multi-bond  $^1\text{H}$ ,  $^{13}\text{C}$  correlation from the C-2  $\text{CH}_2$  to the C-3  $\text{CF}_2$  located at  $^1\text{H}$ ,  $^{13}\text{C} = 2.46$ ,  $118.8$  ppm. This correlation was recorded in a  $^{13}\text{C}$ -detected experiment to obtain a higher digital resolution along the  $^{13}\text{C}$  axis. This multi-bond correlation consists of a set of three major cross peaks, each of which is further split into three distinct 'minor' peaks along the  $^{13}\text{C}$  axis. The spacing between the centers of the three main cross peaks along the  $^{13}\text{C}$  axis is *ca.*  $255$  Hz, corresponding to a  $^1J_{\text{FC}}$ . The separation within each main cross peak is *ca.*  $31.7$  Hz, corresponding to a  $^2J_{\text{FC}}$ . The extra coupling along the  $^{13}\text{C}$  axis arises from an active  $^2J_{\text{FC}}$  coupling of the C-4  $\text{CF}_2$  group with the C-3  $\text{CF}_2$  group. The major cross peaks are split along the  $^1\text{H}$  axis by the  $^3J_{\text{HF}} = 18.7$  Hz coupling, while each set of 'minor' cross peaks is essentially colinear along the  $^1\text{H}$  axis, as no  $J_{\text{HF}}$  coupling can exist between the C-4  $\text{CF}_2$  and the C-3  $\text{CF}_2$ . The modulation of the active AX spins of the C-2  $\text{CH}_2$  by the passive M spins of the C-3  $\text{CF}_2$  is then considered to be a separate three-nucleus interaction that is independent of the effect of the C-4  $\text{CF}_2$ . In this multi-bond correlation, the highest frequency  $^1\text{H}$  cross peak near  $2.50$  ppm has the lowest  $^{13}\text{C}$  frequency near  $117.3$  ppm, and the lowest frequency  $^1\text{H}$  cross peak near  $2.42$  ppm has the highest  $^{13}\text{C}$  frequency near  $120.6$  ppm. The result appears as three cross peaks tilted with a negative slope,

indicating that the relative signs of  $^3J_{\text{HF}}$  and  $^1J_{\text{FC}}$  are unlike.

Because all three heteronuclear couplings are viewed relative to  $^3J_{\text{HF}}$ , and this coupling is common to all three cross peaks, knowledge of the absolute sign of any of the four coupling constants  $^3J_{\text{HF}}$ ,  $^1J_{\text{FC}}$ ,  $^2J_{\text{FC}}$  or  $^1J_{\text{HC}}$  allows the determination of the sign of the other three coupling constants.  $^1J_{\text{FC}}$  is known to be generally of negative sign.<sup>30,31</sup> Figure 5(C) then indicates that  $^3J_{\text{HF}}$  in **1** ought to be assigned a positive sign. Accordingly, since  $^3J_{\text{HF}}$  is common to the other two cross peaks, Fig. 5(B) and (A) indicate that  $^2J_{\text{FC}}$  and  $^1J_{\text{HC}}$  are to be assigned positive signs. The identified heteronuclear coupling constants of **1** are listed in Table 2.

## CONCLUSION

The complexities of interpretation of fluorine-coupled  $^{13}\text{C}$  spectra and lack of straightforward fluorine-decoupling capabilities on commercial NMR instruments have hampered the use of  $^{13}\text{C}$  NMR strategies for the structural analysis of fluorinated molecules. Instead, in many cases  $^{19}\text{F}$  NMR is the only approach used. A full analysis is possible in simple cases. As the number of fluorine nuclei and molecular size increase, both the location and assignment of the fluorine resonances become uncertain. Thus extensive work has been carried out by Weigert and Karel<sup>32</sup> and Bauduin *et al.*<sup>33</sup> to develop calculational models that predict the  $^{19}\text{F}$  NMR chemical shifts for saturated fluorocarbons.

In this work we have combined efficient fluorine decoupling with the  $^{19}\text{F}$ -detected HMQC and HMBC experiments to derive complete  $^{19}\text{F}$  and  $^{13}\text{C}$  assignments in the highly fluorinated alcohol **1**. This represents a new approach with potential for a fuller structural characterization of the carbon backbones of fluorocarbon molecules. Despite broad  $^{19}\text{F}$  lines, we obtained strong  $^{19}\text{F}$ ,  $^{13}\text{C}$  single-bond responses. We did not observe a full complement of  $^{19}\text{F}$ ,  $^{13}\text{C}$  multi-bond correlations. Four groups, C-3, C-4, C-7 and C-8, gave a sufficient number of two-bond  $^{19}\text{F}$ ,  $^{13}\text{C}$  responses to allow the derivation of a full set of assignments. Multi-bond correlations were not detected from the C-5 and

**Table 2.** Several heteronuclear coupling constants in  $\text{CF}_3(\text{CF}_2)_5\text{CH}_2\text{CH}_2\text{OH}^a$

Carbon	$^1J_{\text{HC}}$	$^2J_{\text{HC}}$	$^3J_{\text{HF}}$	$^1J_{\text{FC}}$	$^2J_{\text{FC}}$
C-1	145.2	4.8			
C-2	130.1		18.7		21.2
C-3		3.9	18.7	254.9	31.7
C-7				$\sim 270$	$34.0^b$
C-8				287.2	33.1

<sup>a</sup> Data in Hz at  $28^\circ\text{C}$ . The fluorine-coupled multiplets between  $109$  and  $115$  ppm show  $^1J_{\text{FC}}$  splittings in the range  $264$ – $270$  Hz and  $^2J_{\text{FC}}$  splittings in the range  $31.7$ – $34.4$  Hz for C-4 to C-6, but the multiplets are too complex to assign these splittings.

<sup>b</sup>  $^2J_{\text{FC}}$  from the  $\text{CF}_3$  (C-8) measured when decoupling the  $\text{CF}_2$  fluorine groups.

C-6  $\text{CF}_2$  groups, which show the broadest  $^{19}\text{F}$  signals. Since these groups give strong single-bond responses, it is unlikely that their lack of multi-bond responses is due to a  $T_2^*$  relaxation process. These groups may simply have a different value for the two-bond fluorine-carbon coupling or there may be destructive interference from several values of multi-bond  $^{19}\text{F}$ - $^{13}\text{C}$  couplings.<sup>34</sup> This point needs further investigation as other fluorinated systems are explored. Finally, the 2D strategies illustrated here offer a simple method to obtain the signs

and magnitudes of heteronuclear coupling constants in a complete manner in highly fluorinated systems.

### Acknowledgements

The Duke NMR Center is supported by part by NIH NCI P30-CA-14326. NMR instrumentation in the Duke NMR Center was funded by the NSF, the NIH, the NC Biotechnology Center and Duke University.

### REFERENCES

1. M. A. Hamza, G. Serratrice, M. Stebe and J. J. Delpuech, *J. Am. Chem. Soc.* **103**, 3733 (1981).
2. M. A. Hamza, G. Serratrice, M. Stebe and J. J. Delpuech, *J. Magn. Reson.* **42**, 227 (1981).
3. P. Parhami and B. M. Fung, *J. Phys. Chem.* **87**, 1928 (1983).
4. R. P. Mason, F. M. H. Jeffrey, C. R. Malloy, E. E. Babcock and P. P. Antich, *Magn. Reson. Med.* **27**, 310 (1992).
5. B. Berkowitz, C. A. Wilson, D. L. Hatchell and R. E. London, *Magn. Reson. Med.* **21**, 233 (1991).
6. P. S. Hees and C. H. Sotak, *Magn. Reson. Med.* **29**, 303 (1993).
7. A. A. Ribeiro, *J. Magn. Reson. A* **117**, 257 (1995).
8. A. A. Ribeiro and M. J. Glen, *J. Magn. Reson. A* **107**, 158 (1994).
9. M. Bourdonneau and C. Brevard, *Inorg. Chem.* **29**, 3270 (1990).
10. S. Berger, *J. Fluorine Chem.* **72**, 114 (1995).
11. A. Bax and S. Subramanian, *J. Magn. Reson.* **67**, 565 (1986).
12. M. F. Summers, L. G. Marzilli and A. Bax, *J. Am. Chem. Soc.* **108**, 4285 (1986).
13. A. Bax and M. F. Summers, *J. Am. Chem. Soc.* **108**, 2093 (1986).
14. A. Bax, R. Freeman and G. A. Morris, *J. Magn. Reson.* **42**, 164 (1981).
15. A. Bax and R. Freeman, *J. Magn. Reson.* **44**, 542 (1981).
16. A. Bax and D. G. Davis, *J. Magn. Reson.* **95**, 355 (1985).
17. A. J. Shaka, P. S. Barker and R. Freeman, *J. Magn. Reson.* **64**, 547 (1985).
18. A. J. Shaka, J. Keeler, T. Fienkel and R. Freeman, *J. Magn. Reson.* **52**, 335 (1983).
19. A. J. Shaka, J. Keeler and R. Freeman, *J. Magn. Reson.* **53**, 313 (1983).
20. D. W. Ovenall and R. C. Ferguson, in *Pulse Methods in 1D and 2D Liquid Phase NMR*, edited by W. S. Brey, pp. 489–507. Academic Press, San Diego (1987).
21. A. A. Ribeiro and G. L. Jendrasiak, *Magn. Reson. Chem.* **29**, 482 (1991).
22. J. R. Lyerla, Jr, and D. L. VanderHart, *J. Am. Chem. Soc.* **98**, 1697 (1976).
23. D. W. Ovenall and J. J. Chang, *J. Magn. Reson.* **25**, 361 (1977).
24. A. Bax and R. Freeman, *J. Magn. Reson.* **45**, 177 (1981).
25. V. Rutar, *Chem. Phys. Lett.* **106**, 258 (1984).
26. T. C. Wong, V. Rutar and J. S. Wang, *J. Am. Chem. Soc.* **106**, 7046 (1984).
27. A. L. Cholli, *Appl. Spectrosc.* **45**, 879 (1991).
28. A. L. Cholli, *J. Magn. Reson.* **98**, 589 (1992).
29. A. L. Cholli, *J. Magn. Reson.* **101**, 206 (1993).
30. W. S. Brey and M. L. Brey, in *Encyclopedia of NMR*, edited by D. M. Grant and R. K. Harris, Vol. 3, pp. 2063–2071. Wiley, Chichester (1996).
31. J. Emsley, L. Phillips and V. Wary, *Prog. Nucl. Magn. Reson. Spectrosc.* **10**, 83 (1975).
32. P. J. Weigert and K. J. Karel, *J. Fluorine Chem.* **37**, 125 (1987).
33. G. Bauduin, B. Boutevin and Y. Pietrasanta, *J. Fluorine Chem.* **71**, 39 (1995).
34. M. Salazar, A. S. Zekster and G. E. Martin, *Magn. Reson. Chem.* **25**, 752 (1987).